2013-08-27

A Bond Valence-Based Force Field: A Multi-Body Approach

Matthew Harris Davis
Brigham Young University - Provo

A Bond Valence-Based Force Field: A Multi-Body Approach

Matthew H. Davis

A thesis submitted to the faculty of
Brigham Young University
in partial fulfillment of the requirements for the degree of

Master of Science

Barry R. Bickmore, Chair
Summer Rupper
Jeffrey Humpherys

Department of Geological Sciences

Brigham Young University

August 2013

ABSTRACT

A Bond Valence-Based Force Field: A Multi-Body Approach

Matthew H. Davis
Department of Geological Sciences, BYU
Master of Science

The typical form for a molecular mechanics force field consists of a foundation of pair-wise terms to describe bonded and non-bonded atomic interactions, with multi-body correction terms to deal with the limitations of pair-wise terms. I present here the first attempts of a molecular mechanics model that is founded on multi-body terms, which are based on the Bond Valence Model (Brown, 2002) and recent developments in the Vectorial Bond Valence Model (Bickmore et al., 2013a; Harvey et al., 2006). I calibrated these models on pressure vs. energy curves for a set of SiO_2 polymorphs. The average deviation for the best-fit iteration, with only six adjustable parameters was ±1.98 kcal/mol.

Keywords: bond-valence model, molecular mechanics, vectorial bond-valence model, valence-quadrupole moment

Table of Contents

List of Figures

1 Introduction

The Bond Valence Model (BVM) describes and analyzes chemical structures based on the bond lengths between cations and anions (Brown, 2002). It is mathematically very simple, but usually quantitatively accurate, leading to a robust and intuitive way of interpreting molecular structures in condensed phases. The main requirement in the BVM is that the structural environment of each atom adheres to the "valence sum rule", an adaptation of Pauling's second rule (Pauling, 1929) to account for differences in bond lengths around cations. This rule states that the valence of the bonds incident to an ion should exactly counterbalance the atomic valence, or the oxidation state, of that ion. This simplicity has made the BVM useful in fields ranging from crystallography and inorganic chemistry to molecular biology (Brown, 2002; Brown, 2010).

Simple models, such as the BVM, provide for both computational efficiency and intuitive simplicity over quantum mechanics (Brown, 2003). Chemists often employ simplifications to understand even complex scenarios. For example, Gilbert Lewis presented the idea of Lewis dot structures to help explain differences between polar and non-polar molecules by relating their molecular structures to electronic structures (Lewis, 1916). Among such models, the BVM is not only intuitive, but also powerful in quantitatively predicting certain aspects of molecular structure via the valence sum rule.

The valence of an individual bond between ion *i* and a counterion *j* (s_{ij}) is measured in valence units (v.u.), and is determined using the equation:

$$s_{ij} = e^{\left(\left(R_0 - R_{ij}\right)/B\right)} \tag{1}$$

where R is the bond length, and R_0 and B are constants specific to each cation-anion pair. R_0 is the length of a 1 v.u. bond and B is dependent on the softness of the bond (Adams, 2001). The sign of the bond valence is positive toward the anion and negative toward the cation.

The valence sum, S_i is found by adding all the valences incident to ion i from the surrounding counterions j:

$$S_i = \sum_j s_{ij} \tag{2}$$

If we let V_i represent the atomic valence of ion i, then we can write the valence sum rule as:

$$\Delta S_i = S_i - |V_i| \approx 0 \tag{3}$$

where ΔS_i is the deviation from the ideal valence sum (Brown, 2002).

The valence sum rule (Eq. 3) is useful for predicting acceptable combinations of bond lengths from ligands to a central ion, and is usually quantitatively accurate. Brown (2002) showed that structures that deviate significantly from the valence sum rule are typically strained, thus indicating an energy cost for the deviation. This relationship between structure and energy, inherent in the valence sum rule, could prove useful for analyzing and predicting molecular structures, for example in a molecular mechanics (MM) force field.

MM force fields are based on relationships between structural descriptors and energy, providing a quantitative way of relating the two that is ideally transferable from molecule to molecule. The most important terms in a typical force field are usually pairwise, while less important terms compensate for multi-body effects. I propose that there might be some advantages, therefore, to using BVM-based structural descriptors, which are inherently multi-body. For example, deviation from the valence sum rule (ΔS_i) simultaneously accounts for

interactions between an ion and all of its bonded neighbors. With a force field based primarily on multi-body structural descriptors, we might be able to address some of the shortcomings of typical MM force fields.

This work represents the first attempt to create a force field that employs BVM-based structural descriptors other than ΔS_i. This force field includes a potential energy term based on the valence sum rule to account for bonded interactions, another term based on the recently extended Vectorial Bond-Valence Model (VBVM) to account for spatial distribution of ligands, and a standard van der Waals term for non-bonded interactions. The energy function parameters were optimized to fit several pressure vs. energy curves observed in SiO_2 polymorphs. While some progress was made toward a working force field of this type, this work illuminates areas where this simplest possible model may require further development.

2 Theory

MM force fields are useful for modeling complex molecular interactions at a relatively low computational cost by describing structure-energy relationships with a few terms based on simple geometric descriptors. In the following subsections I describe the form of a typical MM force field and how I have altered it to create a BVM-based alternative.

2.1 A Standard MM Potential Energy Model (Force Field)

The first MM models were presented independently by Hill (1946) and Westheimer and Mayer (1946). Since then, the backbone potential energy terms of most of these models have remained essentially unaltered. A MM force field is typically expressed as the sum of potential energy terms describing interactions between pairs or small sets of atoms. It includes terms to account for bonded and non-bonded interactions (Hinchliffe, 2003; Rappe, 1997). For example,

the ClayFF force field of Cygan et al. (2004), commonly used to model geologic materials, has a form identical to those created more than 60 years ago (Eq. 4).

$$E_{total} = E_{bond\ stretch} + E_{angle\ bend} + E_{VDW} + E_{Coul} \quad (4)$$

In other words, the total potential energy (E_{total}) is the sum of potential energy terms for bond stretching ($E_{bond\ stretch}$) and bond-angle bending ($E_{angle\ bend}$), which are both bonded interactions, as well as terms for van der Waals (E_{VDW}) and electrostatic (E_{Coul}) forces, which are used to account for non-bonded interactions.

2.1.1 Bonded Interactions

As mentioned above, typical force fields account for bonded interactions via bond stretching and bond-angle bending terms. Both of these interactions are sometimes treated as simple harmonic oscillations, but are often given more complex forms.

The bond stretching term for a particular atom *i*, for instance, is sometimes based on Hooke's (1930) Law, taking the form of a second-degree polynomial:

$$E_{bond\ stretch,i} = \sum_j \frac{1}{2} k_{ij} (R_{ij} - R_{e,ij})^2 \quad (5)$$

where k_{ij} is the force constant between atoms *j* incident to atom *i*, while R_{ij} and $R_{e,ij}$ are the measured and equilibrium bond lengths between atom *i* and atoms *j*, respectively. In certain cases, e.g., where bond breaking needs to be modeled, the bond stretching term takes a more complex form, such as the Morse potential (Morse, 1929):

$$E_{bond\ stretch,i} = \sum_j D_{ij} \left(1 - e^{\left(-\propto (R_{ij} - R_{e,ij})\right)}\right)^2 \quad (6)$$

where D_{ij} is the bond energy for the bond between atoms *i* and *j*, and $\propto$ is determined using Eq. 7:

$$\propto = \left[\frac{k_{ij}}{2D_{ij}}\right]^{1/2} \tag{7}$$

where k_{ij} is the "spring" constant between atoms *i* and *j*.

The term for bond-angle bending addresses spatial distribution of ligands by assigning a pair-wise interaction between bonds, rather than atoms. Like the bond stretching term, this term, which accounts for the angle bending energy incident to an atom *B*, is often represented with an adaptation of Hooke's law:

$$E_{angle\ bend,B} = \sum_{AC} \frac{1}{2} k_{ABC} \left(\theta_{ABC} - \theta_{e,ABC}\right)^2 \tag{8}$$

where θ_{ABC} and $\theta_{e,ABC}$ are the measured and equilibrium angles formed by atoms A, B and C respectively, with B as the central atom, and k_{ABC} is the "spring" or force constant. Anharmonic angle-bending terms are also common.

2.1.2 Non-bonded Interactions

Non-bonded interactions are either between similar ions or, if the ions are not similar, they are non-bonded beyond a predefined cutoff radius. For non-bonded interactions, MM force fields often use a Leonard-Jones 6-12 function to account for VDW forces incident to atom *i*, just as Hill (1946) did in his original force field (Eq. 9):

$$E_{VDW,i} = \sum_k D_{ik} \left(\left(\frac{X_{ik}}{R_{ik}}\right)^{12} - 2 \cdot \left(\frac{X_{ik}}{R_{ik}}\right)^{6} \right) \tag{9}$$

Where R_{ik} is the non-bonded distance between each atom pair, *i* and *k*. I chose to treat D_{ik} as the geometric mean of D_i and D_k, constants specific to each atom *i* and *k*, (likewise for X_{ik}), such that:

$$D_{ik} = \sqrt{D_i \cdot D_k} \tag{10}$$

and

$$X_{ik} = \sqrt{X_i \cdot X_k} \tag{11}$$

The first half of Eq. 9 is related to inner-wall repulsion due to electron cloud overlap, while the second half is related to attractive dispersion forces between atoms *i* and *k*.

2.1.3 Other Terms

Other terms such as those used for bond torsion, out-of-plane angle-bending, and atomic or molecular polarizability are used in some force fields, but will not be addressed here. Also, although it has become more common recently to add electrostatic interactions to account for long-range, non-bonded forces, using Coulomb's Law, they were neglected in earlier models (Hinchliffe, 2003), and likewise were omitted for our purposes here.

2.1.4 Shortcomings of typical MM models

One of the main problems with typical force fields is that all the energy terms, or at least the most important ones, are typically pairwise. Treating the chemical environment using pairwise terms is attractive, because we can simply sum all the potential energy terms, two atoms at a time, in a way that is fairly accurate, at least for specific types of chemical scenarios. The problem is that they typically assume some "equilibrium" distance or bond angle that is

determined without regard for the effects of the rest of the bonding environment. For instance, if one bond to a central atom is shorter than average, the equilibrium lengths of the other bonds incident to the same central atom will be affected. Pairwise terms are unable to address this issue without needing to be recalibrated even for different classes of compounds that include the same elements.

Some force fields have a backbone consisting of pairwise terms, but address the aforementioned issue by appending a number of multi-body corrections. However, this results in an increase in both computational expense and the number of adjustable model parameters. Even a model with only two elements can quickly become complicated. Halley et al. (1993) developed a molecular dynamics model to capture the dissociation and polarizability of water. Despite involving only two elements, their model included 21 adjustable parameters, and adding more elements would only increase the expense. Such models are difficult to generalize for different chemical scenarios.

2.2 A BVM-Based Force Field

A force field based on a backbone of intrinsically multi-body terms sidesteps the aforementioned problems. The Valence Sum Rule (Eq. 3), upon which the BVM is based, is inherently multi-body, for instance. Since the sum of the valences must equal the atomic valence, changes to any one bond would alter the other bond lengths to satisfy the rule. Also, the Valence Sum Rule is determined by simply adding pairwise terms, which keeps the computational expense low. Rappe and coworkers have already incorporated energy costs due to ΔS_i into force fields. Cooper et al. (2003) developed a force field calculating potential energy from ΔS_i, long-range Coulombic interactions, and a short-range repulsion term to explain

minimum energy structures of perovskites. They found that geometry optimizations and energy calculations using this force field were comparable to those calculated using density functional theory (DFT). Others applied a similar energy model to metal oxides (Shin, 2005) and to understand ideal structure deviations in perovskites (Grinberg, 2004).

The valence sum rule alone, however, neglects other important structural factors required for a potential energy function. First, it does not account for spatial distribution of ligands since bond valence only addresses cation-anion bond lengths. Second, it does not deal with non-bonded interactions, which are important to allow MM models to have transferrable force constants (Snyder and Schachtschneider, 1965). It might, therefore, be useful to expand the model to encompass these factors in a quantitative manner.

My force field (Eq. 12) included: a potential energy term based on ΔS (Eq. 3) to constrain bond lengths incident to each atom *i* in the formula unit, $E_{VSR,i}$ (Eq. 13), a term based on the concept of vectorial bond valence sums (Bickmore et al., 2013a; Harvey et al., 2006) to constrain the spatial distribution of ligands incident to each atom *i* in the formula unit, $E_{VVS,i}$ (Eq. 18), and a term to describe non-bonded interactions incident to each atom *i* in the formula unit, using a VDW term, $E_{VDW,i}$ (Eq. 9).

$$E_{total,m} = \sum_i E_{VSR,i} + E_{VVS,i} + E_{VDW,i} \quad (12)$$

where *i* is each atom in the formula unit and $E_{total,m}$ is the total energy for each crystal structure, m.

2.2.1 Deviation from the Valence Sum Rule

As previously mentioned, strong deviations from the valence sum rule are typically found in strained structures, implying that bond-stretching energies might be related to deviations from the valence sum rule. Adams et al. (2009) showed that if we assume bond-stretching energies are proportional to the square of ΔS_i, this relationship is equivalent to a Morse potential when individual bonds are isolated. Thus, our proposed $E_{VSR,i}$ term has the form:

$$E_{VSR,i} = \alpha \Delta S_i^2 \tag{13}$$

Where i is each atom in the formula unit, and α is a constant of proportionality and an adjustable parameter.

The value α may be consistent across different atom types and in different sites within a given structure even at different pressures. The work of Zhao et al. (2004) and Angel et al. (2005) showed that variation of bond valence sums with pressure for two different cation sites in several perovskite structures were equivalent, for instance. This consistency across atomic sites makes the valence sum rule useful as a force field term, especially in our pursuit of transferability.

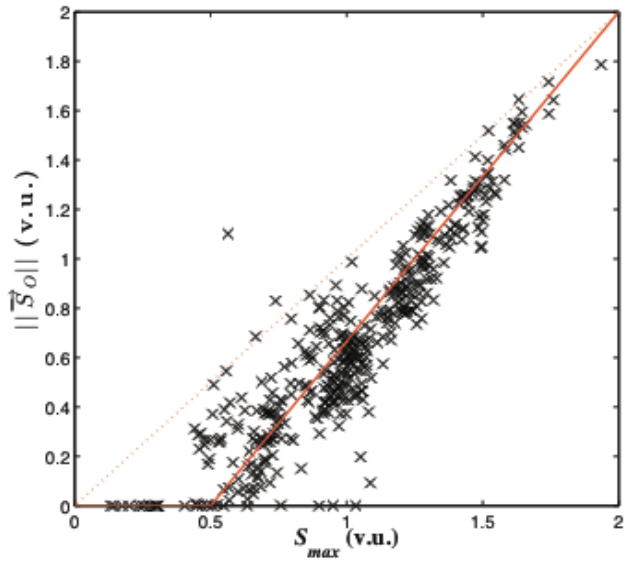

Figure 1 $\|\vec{S}_i\|$ vs. s_{max} for O^{2-} ions in 178 simple oxides. Eq. 14 represents the solid trend line.

2.2.2 Vectorial Bond-Valence Sums

One attempt to describe the coordination sphere by uniting the bond length with spatial distribution of ligands

was that of Harvey et al. (2006), who proposed the application of bond-valence vectors. The vectorial bond valence model (VBVM) or vector sum postulate states that a bond between cation *i* and anion *j*, can be represented by a vector, $\vec{s}_{ij}$, that points from the cation to the anion with a magnitude equal to the bond valence, s_{ij}. Brown (1988) and Harvey et al. (2006) both showed that the sum of these vectors, $\vec{S}_i$, about a given atom *i,* should be approximately zero for stable coordination spheres where electronic structure effects are not present (Eq. 14). This holds true even when the coordination polyhedra are distorted.

$$\vec{S}_i = \sum_j \vec{s}_{ij} \approx \vec{0} \tag{14}$$

Bickmore et al. (2013a) extended the VBVM by showing that geometric distortions of the coordination shell around a central atom due to electronic structure effects (e.g., lone pairs) can be predicted by relating the degree of distortion to the valence of the strongest bond, s_{max} (Eq. 15):

$$s_{max} = \max_j \left\{ e^{\frac{(R_o - R_{ij})}{B}} \right\} \tag{15}$$

Bickmore et al. (2013a) also noted a correlation between $\left\|\vec{S}_i\right\|$ and s_{max} in cases where lone-pair effects cause distortions about, for instance, O^{2-} anions. For example, based on Figure 1, which shows a graph of vectorial valence sums plotted vs. s_{max} for the O^{2-} ions in a collection of 178 simple oxides, they noted that $\left\|\vec{S}_i\right\|$ values seemed to cluster around a line connecting the points (0.5, 0) and (2,2), and suggested that the ideal $\left\|\vec{S}_i\right\|$ for oxygen may be predicted using Eq. 16.

$$\left\|\vec{S}_{O\ (ideal)}\right\| = \begin{cases} \frac{4}{3} s_{max} - \frac{2}{3} & .5 \le s_{max} \le 2 \\ 0 & s_{max} \le .5 \end{cases} \tag{16}$$

Cations should ideally have $\left\|\vec{S}_{c\ (ideal)}\right\| = 0$, unless they are subject to lone-pair or other electronic structure effects. Since the structures used here involve both silicon, which should always have $\left\|\vec{S}_{c\ (ideal)}\right\| = 0$, and oxygen, which is subject to lone-pair effects, deviations from the ideal for atom *i* would then be represented as:

$$\Delta\vec{S}_i = \left\|\vec{S}_{ij}\right\| - \left\|\vec{S}_{i\ (ideal)}\right\| \tag{17}$$

where $\left\|\vec{S}_{i\ (ideal)}\right\|$ is either zero or a function of s_{max}, depending on the central atom. Bickmore et al. noted that outliers tend to be found in unstable or metastable structures, suggesting that deviations from the ideal, $\left\|\vec{S}_{i\ (ideal)}\right\|$, entail some energy cost. From this, and in a similar vein as Eq. 13, I made $E_{VVS,i}$, proportional to the magnitude of $\Delta\vec{S}_i$:

$$E_{VVS,i} = \beta\left|\Delta\vec{S}_i\right| \tag{18}$$

where *i* is each atom in the formula unit, and β is a proportionality constant and another adjustable parameter.

2.2.3 Valence Parameters

As previously mentioned, one of the difficulties with parameterization is that even simple models can quickly become computationally expensive with an increasing number of parameters. Some force fields use chemical rules to reduce the number of parameters that are determined via typical optimization procedures. For example, equilibrium bond lengths can be estimated using atomic radii that are adjusted according to electronegativity or bond order (Rappe, 1997). Some use a united-atoms approach to combine atoms, and therefore parameters, into functional groups (Cramer, 2004). Each of these approaches provides a way of reducing the computational

expense in optimization routines and allows for the addition of more elements without unnecessarily complicating the model.

I used the SoftBV values for R_0 and B (Eq. 1) of Adams et al. (2001) to reduce the number of adjustable parameters in this simplified model. It is important to note though that these parameters have been optimized for a large number of stable crystal structures by assuming only the valence sum rule (Eqn. 3) and thus represent averages. This means that they ultimately should be optimized in future models, but to keep this model simple, I kept them constant.

2.2.4 Non-Bonded Interactions

I used the Leonard-Jones 6-12 function (Eq. 9) to represent the $E_{VDW,i}$ term. For SiO_2 this term has four total parameters, D_i and X_i for each atom i, and D_k and X_k for each atom k, such that when atom i and k interact, the resultant D_{ik} and X_{ik} (Eqs. 10 & 11) represent three types of interactions: Si-Si, O-O and Si-O. These parameters were originally set to the values taken from the Universal Force Field (UFF) (Rappe et al., 1992), but later were made adjustable.

3 Methods

Typical MM models have similar forms from one model to the next, and so only differ in the parameter values determined via optimization techniques. The model presented here has a similar form to typical MM models, except that I replaced the standard pairwise bonded interaction terms with multi-body terms based on valence sums and valence vector sums, and I incorporated only a van der Waals term to explicitly account for non-bonded interactions.

My parameterization strategy consisted of four parts—1) collecting data on which to calibrate the models, 2) determining which model parameters to treat as adjustable, 3) optimizing

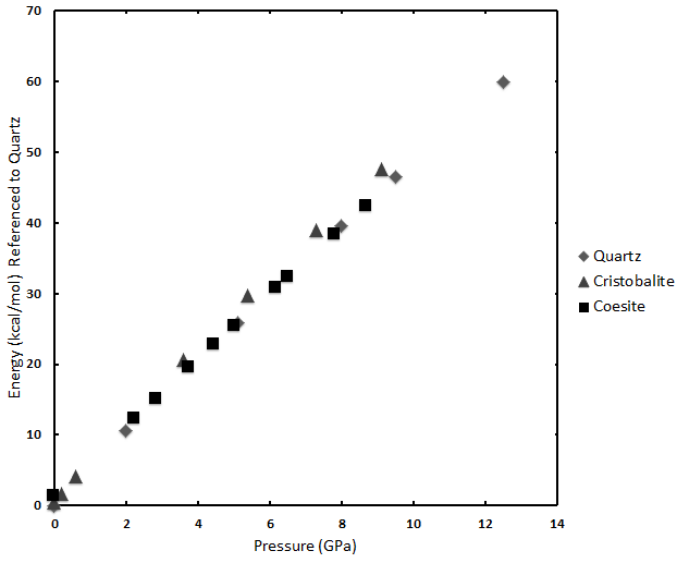

Figure 2 Pressure vs. energy plots for 3 polymorphs of SiO2. Each polymorph's energy has had the initial ΔG value for quartz subtracted from them.

the adjustable parameters, and 4) comparing the model to empirically determined structure-energy data.

3.1 Data

Since a force field such as this relates molecular structure to potential energy, any parameterization scheme must involve known molecular structures, for which something is known about the potential energies. In this case, I used SiO_2 crystal polymorphs, in individual pressure series, of quartz (Hazen et al., 1989), coesite (Angel et al., 2003), cristobalite (Dera et al., 2011; Downs and Palmer, 1994), and stishovite (Yamanaka et al., 2002). I first calculated each unit cell volume (V) based on unit cell size, then fit a third-degree polynomial to relate V with pressure (P), which I integrated to determine Gibbs free energy (assuming a constant temperature) according to the equation:

$$\int_{P_0}^{P} V dP = \Delta G \qquad (19)$$

where ΔG represents the change in Gibbs energy from an initial pressure, P_0, to a final pressure, P. I used these values to plot pressure vs. energy in Figure 2, which was normalized by subtracting quartz at STP (Robie et al., 1978) from each energy value.

3.2 Adjustable Parameters

At its simplest, my model initially had only three adjustable parameters—α (from Eq. 13, a single value for both Si and O), β (from Eq. 18, where β was the same for both Si and O as well) and I initially kept D_{ik} and X_{ik} constant (using UFF parameters). I applied a scaling factor, γ, to the VDW term to account for unit conversions and for computational efficiency. I later omitted γ, since it's simply an across-the-board adjustment to D_{ik} (see Eq. 9) and made D_i and X_i adjustable, for a total of six parameters. α, β and γ were all constrained to be between .0001 and 10^5, while D_i and X_i were constrained to be between .0001 and 10.

3.3 Optimization

I carried out optimization using a combination of the GRG Nonlinear Solver in Microsoft Excel and the *multistart* function in the MATLAB Global Optimization Toolbox, in conjuction with the *fmincon* function in the MATLAB Optimization Toolbox. Since most of my model terms (e.g., interatomic distances, bond valences, and bond-valence vectors) were constant, I created a script that preallocated these values into a database, which I used to optimize my adjustable parameters. (All MATLAB programs are available upon request from the author). The goal of optimization was to minimize the error function:

$$\epsilon = \sum_m (E_{total\,m} - E_{Gibbs\,m})^2 \qquad (20)$$

where $E_{total\,m}$ is the total energy (per mole of SiO_2 formula units) for each crystal structure, m, and $E_{Gibbs\,m}$ is the Gibbs free energy for the same crystal structure, m, calculated using Eq. 19. As previously mentioned, each of these energies was referenced to quartz and was optimized on the structure-energy relationships ($E_{Gibbs\,m}$) of quartz and coesite.

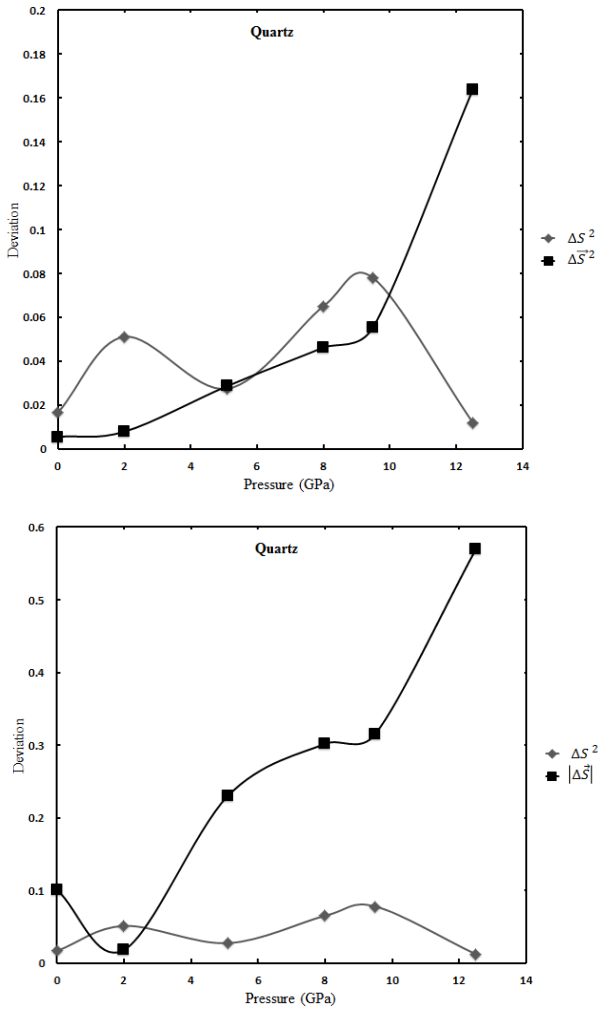

Figure 3 Pressure vs. deviation from ideal values for both VSR and VVS for Quartz. After removing the square, VVS now nearly mirrors the VSR.

3.4 Model Testing

To assess the quality of the optimized parameters, I first fit them to the quartz and coesite pressure series together, then used those values to calculate energies for the cristobalite pressure series. I then calculated cristobalite's average deviation from the Gibbs free energies to see if it was similar to the deviations for quartz and coesite. I also used the parameters to calculate energies for stishovite structures, but since these are based on highly distorted SiO_6^{8-} octahedra, rather than SiO_4^{4-} tetrahedra, we did not expect good results (see Section 4.1 below).

4 Results/Discussion

With optimization, factors such as the initial value and each parameter's constraints are vital for ensuring a global minimum. Understanding the reasonableness of parameter values helps to target the range of ideal values for parameterization. Also, each optimization run helped to shape future iterations. Those parameters which were continually forced to zero or to the bounds of the constraints in an optimization run, illuminated possible issues with each term or even portions of terms in my model. For example, the β term (Eq. 18) initially began as the deviation from ideal vectorial bond valence sums squared, but with each optimization, the α term

(Eq. 13) would continually be forced to zero as the β term was not able to balance out the oscillations of the α term's energy with increasing pressure, especially noticed in the structures of quartz and coesite. It wasn't until I changed the β term to an absolute deviation that it balanced the α term's energies (Figure 3), α was no longer forced to zero, and the model produced better fits. This was only one of many changes, and the following sections represent the ultimate result of these iterations.

4.1 Three Parameters

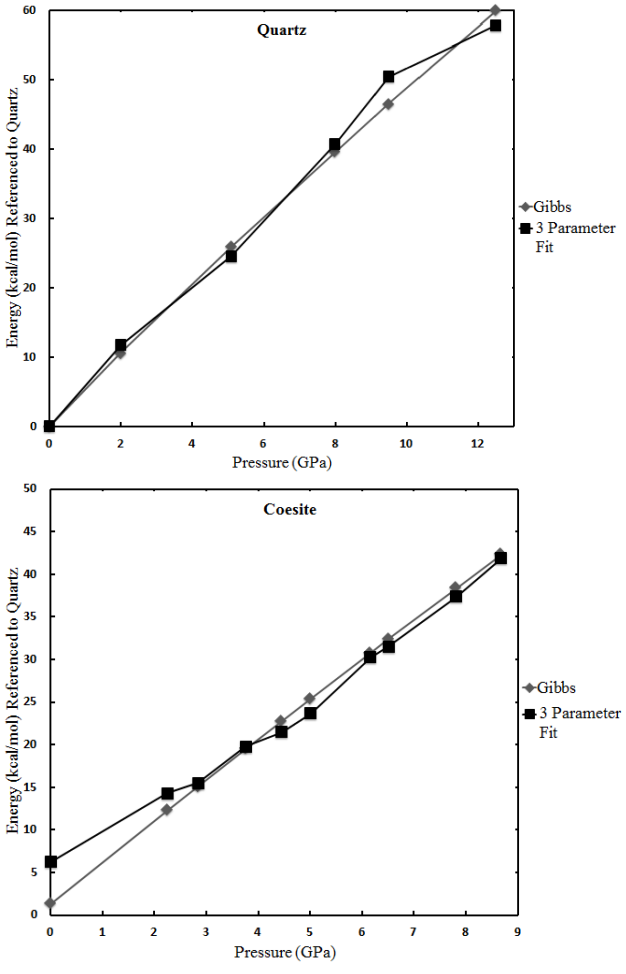

Figure 4 Pressure vs. energy calculations (based on 3 parameters) for quartz and coesite with corresponding Gibbs energy plots (see figure 2).

The three-parameter model resulted from several optimization iterations in which I had split α and β up for Si and O. Each time they were divided, they were either zeroed out, possibly indicating the optimization finding individual atoms values to be too chaotic, or they were so similar that it appeared they would be better as a single parameter.

As previously mentioned, I fit the model parameters to the pressure vs. energy curves for quartz and coesite, the graphs of which are given in figure 4, with the parameters of best fit α=175.57 kcal/mol/v.u.^{2}, β=51.96 kcal/mol/v.u. and

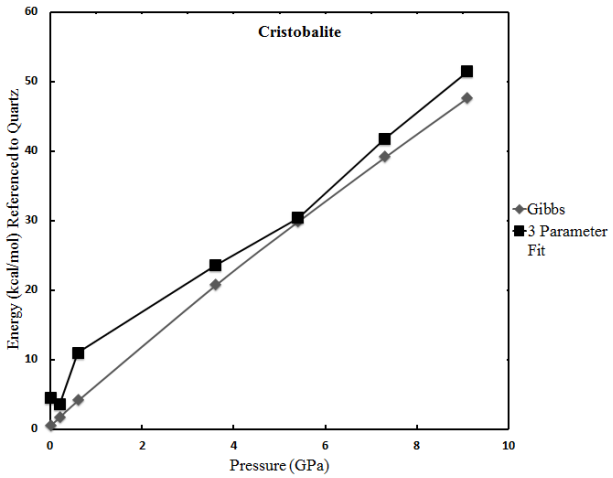

Figure 5 Pressure vs. energy calculations for cristobalite using quartz and coesite parameters, with corresponding Gibbs energy plots (see figure 2).

γ=0.385 (see Eq. 12). The average deviation for these two polymorphs was ±1.93 kcal/mol. I used these parameters in the model to calculate energies for the cristobalite structures, which yielded an average deviation of ±3.76 kcal/mol (see figure 5) for cristobalite alone. I also used the same parameters for stishovite, but the fits were poor (129.44 kcal/mol) which may be due to the fact that Si in stishovite is 6-coordinated, and some correction based on coordination number appears to be needed in a future model.

A possible route for a more generalized model could be to include a term based on the valence quadrupole moment (Bickmore et al., 2013b), which is more likely to describe distortions in coordination octahedra than the valence vector sum. The valence quadrupole is essentially the next term in a monopole expansion of the spatial distribution of bond valence about each atom. The valence sum is a zeroth-order tensor, or monopole moment, that describes the total bond valence incident to an atom. The vectorial valence sum is a first-order tensor, or a dipole moment, that describes the lopsidedness of the bond valence distribution incident to each central atom. The valence quadrupole moment (VQM) is a second-order tensor that describes the sphericity of the bond valence distribution (Bickmore et al., 2013b). This provides another quantitative measure of the degree of distortion of the bonding environment incident to a particular atom. Some distortion modes of octahedra, for instance, have no effect on the vectorial valence sum, but have a large effect on the VQM. As research is still new in this area,

including a VQM term in my force field was not feasible, but may be valuable to incorporate into future models.

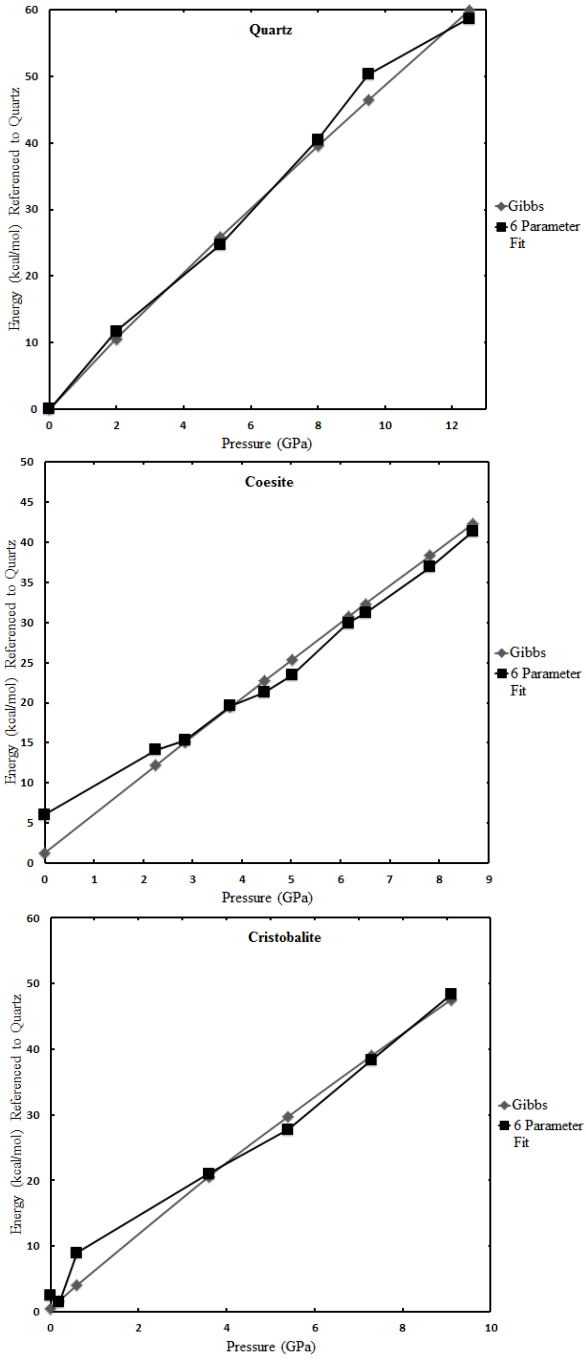

Figure 6 Pressure vs. energy calculations (based on 6 parameters) for quartz, coesite and cristobalite with corresponding Gibbs energy plots (see figure 2).

4.2 Six Parameters

When I optimized Eq. 20 with six parameters, I obtained: $\alpha = 157.657$ kcal/mol/v.u.^{2}, $\beta = 50.384$ kcal/mol/v.u., $X_{Si} = 7.737$ Å, $X_O = 5.944$ Å, $D_{Si} = .0001$ kcal/mol, $D_O = .0001$ kcal/mol. This optimization was similar to the three parameters (see Figure 6), with the quartz and coesite average deviation decreasing to ±1.876 kcal/mol and the cristobalite average deviation decreasing to ±2.197 kcal/mol. It is interesting to note that D_{Si} and D_O were forced to their lower bounds, which may be due to the model's attempt to force van der Waals interactions to be predominately repulsive. It may be beneficial in future models to consider splitting up the van der Waals attractive and repulsive terms, instead of leaving them combined in a Lennard-Jones potential, or using only the repulsive portion of this potential.

This may allow us to reduce the number of adjustable model parameters.

5 Conclusions

There is great power in the simplicity and quantitative accuracy of the BVM. By fitting our model with only three parameters to quartz and coesite, my force field was able to describe the evolution of cristobalite's energy with pressure reasonably accurately. I was also able to slightly improve the fit for cristobalite by making the van der Waals parameters adjustable, for a total of six parameters. These parameters proved to be transferrable to three different crystal structures based on SiO_4^{4-} tetrahedra: quartz, coesite, and cristobalite. Also, this model was able to describe pressure series calculations over a large range of pressures (changes representing nearly 400 km depth beneath the Earth's crust) with only small deviations (average deviations of ±1.98 kcal/mol, the maximum deviation being <5kcal/mol for a single value in cristobalite), much less than expected. Even typical quantum mechanical (density functional theory) calculations applied to a single SiO_2 polymorph crystal structure can easily deviate from one another by ±50 kcal/mol between models, depending on the approximations and assumptions employed (Demuth, 1999). My model also produced curves with crossovers for quartz and coesite at pressures close to those found at their normal phase transitions, with cristobalite never becoming the stable phase, as expected (see Figure 7). While a model that reasonably represents these three polymorphs of SiO_2 over such a large pressure range is an important step forward, more work is required to develop a more universal force field that, e.g., is able to model changes in coordination number, and exhibits improved accuracy.

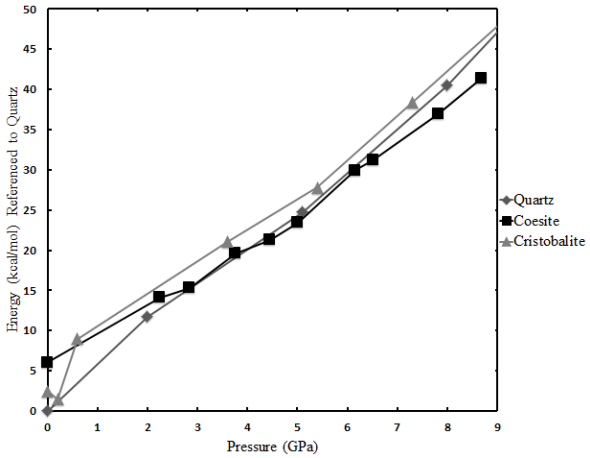

Figure 7 Pressure vs. calculated energy curves (using 6 parameters) for quartz, coesite and cristobalite. The relative energies are fairly consistent with observed phase transitions.

There are several ways in which the model presented here might be improved. First, further research is necessary with valence quadrupole moments as they may lead to more generalized model terms, and may better handle changes in coordination number. Second, an electrostatic term was omitted in this particular model due to the poor fits obtained when it was included in the initial optimizations. This may need to be incorporated in future models as van der Waals may not be sufficient to describe all non-bonded interactions, or it may be that any extra non-bonded terms may need to be limited or even removed altogether if the α, β and VQM terms sufficiently model the non-bonded atomic interactions. Third, as previously mentioned, the valence parameters R_o and B should be optimized to account for interactions other than those only in the valence sum term. Fourth, the VDW term may need to be divided so that each interaction may be treated separately, i.e., so that each interaction (Si-Si, O-O, and Si-O) has a unique D and X rather than assuming the D and X values for Si-O interactions are the geometric averages of those for Si-Si and O-O interactions. Fifth, it may be feasible to only use attractive or repulsive terms for certain interactions.

Another consideration is the lack of data on which future models can be optimized. While this sample size was sufficient for a model with so few parameters, adding more parameters to the model would necessitate the supplementation of more data points to be considered robust. Since the number of crystal structures available is limited, it would be beneficial in future optimizations to utilize quantum mechanical calculations of non-equilibrium

structures, where atoms can be arbitrarily moved in diverse configurations, to better constrain how each term competes with the others to account for the total energy. Notwithstanding all of these limitations, this work shows promise that a molecular mechanics model with transferable energy parameters using multi-body bond valence terms may be possible, and illuminates possible areas for improvement in relating bond valence structural descriptors to energy.

References

Adams, S., 2001, Relationship between bond valence and bond softness of alkali halides and chalcogenides: Acta Crystallographica Section B-Structural Science, v. 57, p. 278-287.

Adams, S., and Rao, R. P., 2009, Transport pathways for mobile ions in disordered solids from the analysis of energy-scaled bond-valence mismatch landscapes: Physical Chemistry Chemical Physics, v. 11, no. 17, p. 3210-3216.

Andrews, D. H., 1930, The relation between the Raman Spectra and the structure of organic molecules: Physical Review, v. 36, no. 3, p. 544-554.

Angel, R. J., Ross, N. L., and Zhao, J., 2005, The compression of framework minerals: European Journal of Mineralogy, v. 17, no. 2, p. 193-199.

Angel, R. J., Shaw, C. S. J., and Gibbs, G. V., 2003, Compression mechanisms of coesite: Physics and Chemistry of Minerals, v. 30, no. 3, p. 167-176.

Bickmore, B. R., Shepherd, K., Johansen, J., Goodell, T., Wander, M. C. F., Davis, M., Andros, C., Lind, L., and Robertson, K., 2013b, Electronic structure effects in the vectorial bond-valence model: The valence quadrupole moment: Provo, UT, Brigham Young University.

Bickmore, B. R., Wander, M. F. C., Edwards, J., Maurer, J., Shepherd, K., Meyer, E., Johansen, W. J., Frank, R. A., Andros, C., and Davis, M., 2013a, Electronic structure effects in the vectorial bond-valence model: American Mineralogist, v. 98, no. 2-3, p. 340-349.

Brown, I. D., 1988, What factors determine cation coordination numbers?: Acta Crystallographica, v. B44, p. 545-553.

Brown, I. D., 2002, The chemical bond in inorganic chemistry: The bond valence model, New York, Oxford University Press, 278 p.:

Brown, I. D., 2010, Recent developments in the methods and applications of the bond valence model: ChemInform, v. 41, no. 13, p. no-no.

Brown, T. L., 2003, Making truth: Metaphor in science, Urbana-Champaign, University of Illinois Press, 215 p.:

Cooper, V. R., Grinberg, I., and Rappe, A. M., 2003, Extending first principles modeling with crystal chemistry: a bond-valence based classical potential: AIP Conference Proceedings, v. 677, no. 1, p. 220.

Cramer, C. J., 2004, Essentials of computational chemistry : theories and models, Chichester, West Sussex ; Hoboken, NJ, J. Wiley, xx, 596 p. p.:

Cygan, R. T., Liang, J.-J., and Kalinichev, A. G., 2004, Molecular models of hydroxide, oxyhydroxide, and clay phases and the development of a feneral force field: The Journal of Physical Chemistry B, v. 108, no. 4, p. 1255-1266.

Demuth, T., Jeanvoine, Y., Hafner, J., and Angyan, J. G., 1999, Polymorphism in silica studied in the local density and generalized-gradient approximations: Journal of Physics: Condensed Matter, v. 11, no. 19, p. 3833-3874.

Dera, P., Lazarz, J. D., Prakapenka, V. B., Barkley, M., and Downs, R. T., 2011, New insights into the high-pressure polymorphism of SiO2 cristobalite: Physics and Chemistry of Minerals, v. 38, no. 7, p. 517-529.

Downs, R. T., and Palmer, D. C., 1994, The pressure behavior of alpha-cristobalite: American Mineralogist, v. 79, no. 1-2, p. 9-14.

Grinberg, I. C., Valentino R.; Rappe, Andrew M., 2004, Oxide chemistry and local structure of PbZrxTi1-xO3 studied by density-functional theory supercell calculations: Physical Review B, v. 69, p. 144118.

Halley, J. W., Rustad, James R., Rahman, A., 1993, A polarizable, dissociating molecular dynamics model for liquid water: The Journal of Chemical Physics, v. 98, no. 5, p. 4110-4119.

Harvey, M. A., Baggio, S., and Baggio, R., 2006, A new simplifying approach to molecular geometry description: the vectorial bond-valence model: Acta Crystallographica, no. B62, p. 1038-1942.

Hazen, R. M., Finger, L. W., Hemley, R. J., and Mao, H. K., 1989, High-pressure crystal-chemistry and amorphization of alpha-quartz: Solid State Communications, v. 72, no. 5, p. 507-511.

Hill, T. L., 1946, On steric effects: The Journal of Chemical Physics, v. 14, no. 7, p. 465-465.

Hinchliffe, A., 2003, Molecular modelling for beginners, Manchester, John Wiley & Sons Ltd., 410 p.:

Lewis, G. N., 1916, The atom and the molecule: Journal of the American Chemical Society, v. 38, no. 4, p. 762-785.

Morse, P. M., 1929, Diatomic molecules according to the wave mechanics. II. Vibrational levels: Physical Review, v. 34, no. 1, p. 57-64.

Pauling, L., 1929, The principles determining the structure of complex ionic crystals: Journal of the American Chemical Society, v. 51, p. 1010-1026.

Rappe, A. K., Casewit, C. J., Colwell, K. S., Goddard, W. A., and Skiff, W. M., 1992, UFF, a full periodic-table force-field for molecular mechanics and molecular-dynamics simulations: Journal of the American Chemical Society, v. 114, no. 25, p. 10024-10035.

Rappe, A. K., Casewit, Carla J., 1997, Molecular mechanics across chemistry, Sausalito, CA, University Science Books, xii, 444 p. p.:

Robie, R. A., Hemingway, B. S., and Fisher, J. R., 1978, Thermodynamic properties of minerals and related substances at 298.15K and 1 bar (10^5 pascals) pressure and at higher temperatures, Washington, U.S. Govt. Print. Off., Geological Survey bulletin 1452, iii, 456 p. p.:

Shin, Y.-H. C., Valentino R.; Grinberg, Ilya; Rappe, Andrew M., 2005, Development of a bond-valence molecular-dynamics model for complex oxides: Physical Review B, v. 71, no. 5.

Snyder, R. G., and Schachtschneider, J. H., 1965, A valence force field for saturated hydrocarbons: Spectrochimica Acta, v. 21, no. 1, p. 169-195.

Westheimer, F. H., and Mayer, J. E., 1946, The theory of the racemization of optically active derivatives of diphenyl: The Journal of Chemical Physics, v. 14, no. 12, p. 733-738.

Yamanaka, T., Fukuda, T., and Tsuchiya, J., 2002, Bonding character of SiO2 stishovite under high pressures up to 30 Gpa: Physics and Chemistry of Minerals, v. 29, no. 9, p. 633-641.

Zhao, J., Ross, N. L., and Angel, R. J., 2004, New view of the high-pressure behaviour of GdFeO3-type perovskites: Acta Crystallographica Section B-Structural Science, v. 60, p. 263-271.